Multiplet effects in the Ru $L_{2,3}$ x-ray-absorption spectra of Ru(IV) and Ru(V) compounds

Z. Hu, H. von Lips, M. S. Golden, and J. Fink
Institute for Solid State Research, IFW Dresden, D-01171 Dresden, Germany

G. Kaindl
Institut für Experimentalphysik, Freie Universität Berlin, Arnimallee 14, D-14195 Berlin-Dahlem, Germany

F. M. F. de Groot
Department of Inorganic Chemistry, University of Utrecht, Sorbonnelaan 16, 3584 CA Utrecht, The Netherlands

S. Ebbinghaus and A. Reller
Institut für Anorganische und Angewandte Chemie, Universität Hamburg, Martin-Luther-King-Platz 6, 20146 Hamburg, Germany

We report combined experimental and theoretical investigations of x-ray absorption at the Ru-$L_{2,3}$ and O-K thresholds of the Ru(IV) compounds RuO_2 and Sr_2RuO_4 and of the Ru(V) compound $Sr_4Ru_2O_9$. Significant differences in the intensity distribution of the t_{2g}-related and e_g-related peaks between the L_3 and the L_2 edges are found, due to the combined effects of $4d$ spin-orbit coupling and the interelectronic Coulomb interaction described by the Slater integrals. The observed spectral features can be well reproduced by crystal-field-multiplet calculations. With increasing the Ru valence from IV to V, the spectra are shifted by $\cong 1.5$ eV to higher energy at the Ru-$L_{2,3}$ edges and $\cong 1.0$ eV to lower energy at the O-K edge, which is of the same order of magnitude as on going from the divalent to the trivalent late $3d$ transition-metal oxides.

I. INTRODUCTION

Correlation effects are well known in the x-ray absorption spectra (XAS) of the $3d$ transition-metal (TM) L_2 and L_3 edges, and can be well reproduced using crystal-field-multiplet calculations (CFMC) by combining atomic multiplet programs with group theory in a crystal field.[1,2] In contrast, it has often been assumed that the $L_{2,3}$ spectra of the $4d$ TM compounds reflect directly unoccupied $4d$ orbitals influenced by the local symmetry of the metal ion, and spectra have been interpreted in terms of crystal-field or molecular-orbital theories.[3–6] In this context, the single peak observed at the Ru-L_2 edge and the two peaks at the Ru-L_3 edge of $Ru(NH_3)_6Cl_3$ (which has a Ru $4d^5$ configuration and octahedral symmetry) were explained in terms of vanishing matrix elements for the transitions at the L_2 edge into the t_{2g} orbitals resulting from consideration of the $4d$ spin-orbit coupling within a single-particle treatment.[7] On the other hand, detailed CFMC resulted in multiplet spectra with a single peak at the L_2 and a double peak at the L_3 edge for a $4d^5$ configuration.[8] Thus, both the $4d$ spin-orbit and the CFMC approaches can account for the XAS data of $4d^5$ systems.

The differences between the two theoretical approaches become interesting in the case of a $4d^4$ system. In this case, the $4d$ spin-orbit argumentation used in Ref. 7 predicts that a $4d^4$ compound should have the same single peak at the L_2 edge as is the case for $4d^5$. In contrast, CFMC calculations predict a double-peaked structure at both the L_2 and L_3 edges.[8] Thus it is unclear to what extent the single-particle treatment or the CFMC approach represents the correct theoretical background in which to rationalize the experimental $L_{2,3}$ XAS spectra in $4d$ electron systems.

The experimental study of $4d^4$ systems such as Ru(IV) could provide vital information in the solution of this problem. This point forms part of the motivation behind the work presented in this paper: We have studied the Ru-$L_{2,3}$ XAS spectra of two $4d^4$ compounds RuO_2 and Sr_2RuO_4. The latter is also of additional interest in the context of parallels with La_2CuO_4, both structurally and as regards superconductivity ($T_c = 0.93$ k for Sr_2RuO_4).[9] Furthermore, the coexistence of superconductivity and magnetic order was recently found in $R_{2-x}Ce_xRuSr_2Cu_2O_{10}$ (R is a trivalent lanthanide element).[10,11] As both Ru and Cu can support different valence states [Ru(IV/V), Cu(II/III)], the question of their valency in these materials (even without Ce doping) requires clarification. Nevertheless, it has been assumed that Ru is pentavalent in these compounds.[10] As a better understanding of these highly complex materials is desirable, it is of importance first to investigate a more simple Ru(V) system. This forms the second aim of this paper, in which the Ru-$L_{2,3}$ XAS spectrum of $Sr_4Ru_2O_9$ [Ru(V), $4d^3$] is used to set up a Ru(V) reference system for future work on the more complex $R_{2-x}Ce_xRuSr_2Cu_2O_{10}$ systems.

We will show that the significant difference between the spectral features of the L_2 and L_3 edges for Ru systems with $4d^4$ and $4d^3$ configurations, the details of the spectral form for both configurations as well as the energy shift from Ru(IV) to Ru(V) can be well reproduced by the calculations within the CFMC approach, thus confirming the importance of the correlation effects in the $L_{2,3}$ absorption edges of $4d$ TM systems such as the Ru materials considered here.

II. EXPERIMENT

The Ru-$L_{2,3}$ XAS spectra of polycrystalline RuO_2, Sr_2RuO_4 and $Sr_4Ru_2O_9$ were recorded in transmission geom-

etry at the EXAFS-II beamline of HASYLAB/DESY in Hamburg, using a Si(111) double-crystal monochromator. This resulted in an experimental resolution of $\cong 1.2$ eV (full width at half maximum) at the Ru-L_3 threshold (2838 eV). A linear background was subtracted from the measured spectra. The O-K XAS measurements were recorded in fluorescence-yield mode with an escape depth of 2000 Å at the SX700/II monochromator operated by the Freie Universität Berlin at the Berliner Elektronenspeicherring für Synchrotronstrahlung (BESSY I). The experimental resolution at the O-K threshold was 0.3 eV and the data were corrected for the energy-dependent incident flux. The spectra were measured at normal incidence with the fluorescence photons being detected at 40° from the surface normal. The data have been corrected for the energy-dependent incident flux and for self-absorption effects according to a procedure described elsewhere.[12,13]

The Sr_2RuO_4 were prepared in the Universität Hamburg.[14] A Rietveld refinement calculation of the x-ray diffraction (XRD) diagram was carried out to determine its crystal structure. All parameters showed deviations of less than 1% from the structural data given by Ref. 15. $Sr_4Ru_2O_9$ was prepared of the Université de Bordeaux and its characterization by single-crystal x-ray diffraction is described in Ref. 16. To determine the oxidation states of the three compounds studied in this work it was essential to measure their oxygen contents. Therefore we have carried out thermogravimetric investigations: The samples were reduced in a H_2/N_2 atmosphere and from the measured weight loss the oxygen stoichiometry was calculated. It turned out that all three compounds showed the expected oxygen stoichiometry within the method's typical error of ± 0.02. No detectable change in phase purity, etc., was found in the compounds after the O-K XAS measurements were carried out.

III. EXPERIMENTAL RESULTS AND DISCUSSION

The Ru ions in the three compounds studied have basically an octahedral coordination and therefore experience a crystal field with O_n symmetry resulting in the splitting of the $4d$ states into $t_{2g}(d_{xy},d_{xz},d_{yz})$ and e_g $(d_{z^2},d_{x^2-y^2})$ levels separated by $\Delta = 10$ Dq. In general, within the single-particle model two peaks are expected at both the L_2 and L_3 edges corresponding to $2p \rightarrow t_{2g}$ and $2p \rightarrow e_g$ transitions for the configuration d^0 to d^5 (we neglect here the weak $2p \rightarrow ns$ transition, $n \geq 5$). For the configurations d^6 to d^9, the $2p \rightarrow t_{2g}$ channel is closed, and a single peak related to $2p \rightarrow e_g$ transitions is expected. However, upon consideration of the $4d$ spin-orbit coupling, the transitions to some of the crystal-field-split orbitals become forbidden. Figure 1 shows schematically an energy-level diagram of the $4d$ orbitals as they successively experience (i) an octahedral field, (ii) a spin-orbit splitting, and (iii) a weak tetragonal distortion. Forbidden transitions marked with ''XX'' are obtained by calculations of the transition matrix elements using the crystal-field-orbital wave functions, $\Gamma_8^{1,2}, \Gamma_8^{3,4}, \Gamma_7^{1,2}, \Gamma_8^{1,2}, \Gamma_8^{3,4}$, listed here in order of increasing energy.[7] From Fig. 1, one can predict that, within this single-particle spin-orbit scenario, at the L_2 edge the $2p \rightarrow t_{2g}$ channel is closed for $4d$ occupation equal to or exceeding four electrons, and only one peak is expected in the L_2 x-ray absorption spec-
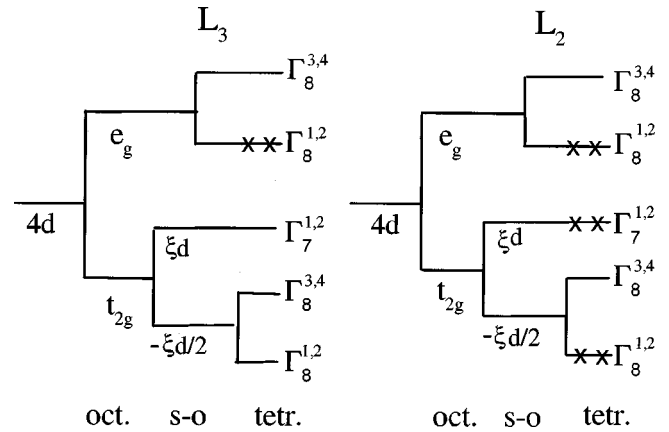

FIG. 1. Schematical energy-level diagram of the $4d$ orbitals (after Ref. 7) as they successively experience an octahedral field, a spin-orbit splitting, and a weak tetragonal distortion. The forbidden transitions at both the L_2 and L_3 edges are marked with ''XX'' (for details see text).

trum. As was mentioned earlier, this is experimentally found to be the case for the $4d^5$ configuration present in the Ru(III) systems $Ru(NH_3)_6Cl_3$ and K_3RuCl_6.[4,7] We now turn our attention to the experimental situation for $4d^4$ systems. The L absorption edges of the Ru(IV) systems RuO_2 and Sr_2RuO_4 as well as the Ru(V) system $Sr_4Ru_2O_9$ are shown in Fig. 2 (the latter will be dealt with later). To ease comparison, the L_2 spectra (open symbols) have been shifted in each case such that the high energy feature (B) is aligned with the corresponding feature in the L_3 spectra (filled symbols). The L_2 spectra have also been multiplied, in the case of both $4d^4$ systems, by a factor of 2.15. The spectra of the Ru $4d^4$ systems exhibit two peaks (denoted as A and B), at both the L_3 and L_2 edges. The lower energy peak A and the higher energy peak B can be basically assigned to $2p \rightarrow t_{2g}$ and
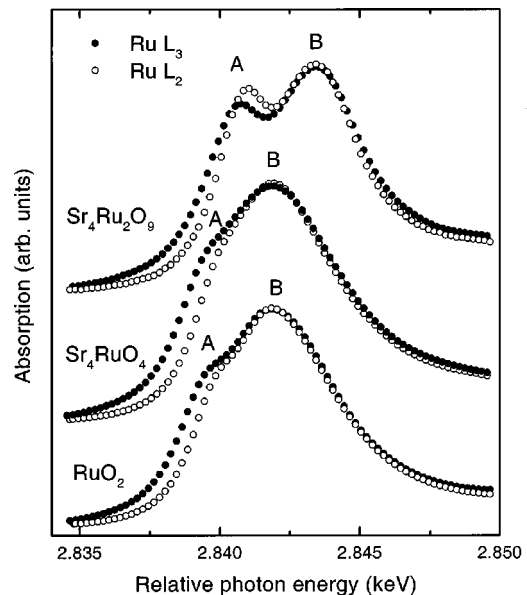

FIG. 2. Measured Ru-L_2 (open symbols) and Ru-L_3 (filled symbols) XAS spectra of the Ru(IV) compounds RuO_2, Sr_2RuO_4, and the Ru(V) compound $Sr_4Ru_2O_9$. For comparison, the Ru-L_2 edge is shifted to overlap the Ru-L_3 edge at the peak B and is multiplied by 2.15 and 2.0 for the Ru(IV) and Ru(V) compounds, respectively.

$2p \rightarrow e_g$ transitions, respectively. The observed spectral features thus clearly indicate that the $2p \rightarrow t_{2g}$ excitation channel is not closed at the Ru-L_2 edge for the $4d^4$ configuration, indicating that the single-particle approach illustrated in Fig. 1 is certainly not the whole story. What is missing in this approach is an adequate treatment of the $2p/4d$ correlation effects. For $3d$ TM compounds these effects are comparable with the spin-orbit coupling of the $2p$ core hole, resulting in a strong transfer of intensity between the L_2 and L_3 edges, and are also stronger than the crystal-field splitting, resulting in a more complex multiplet structure. For the $4d$ TM elements, the $2p/4d$ coupling amounts to $\cong 2$–3 eV, and is thus much smaller than the spin-orbit splitting of the $2p$ level (larger than 100 eV), and consequently the correlation effects have no influence on the L_3 and L_2 intensity ratio. However, the $2p/4d$ coupling is of the same magnitude as the crystal-field strength (10Dq) and can therefore result in a transfer of intensity between t_{2g}-related and e_g-related final states. It should also be noted that although the $4d/4d$ multiplet interaction and the $4d$ spin-orbit coupling are one order of magnitude smaller than the crystal-field strength, they determine the symmetry of the wave functions of the $4d$ state, thus in turn determining the intensity of the transitions. Thus, bearing in mind that the L_2 data for the Ru(IV) systems shown in Fig. 2 are already multiplied by 2.15 in order to match the intensity of the L_3 spectra at feature B, the combined effects of correlation and the $4d$ spin-orbit coupling lead to the observed suppression of the t_{2g}-related L_2 spectral weight for both RuO$_2$ and Sr$_2$RuO$_4$ in comparison with the analogous feature in their L_3 edges.

We now turn to the Ru(V) compound Sr$_4$Ru$_2$O$_9$, which has a $3d^3$ configuration. From Fig. 1 (single-particle model) we would expect that the t_{2g}:e_g ratio is smaller at the L_2 than at the L_3 edge, because of the forbidden nature of the transition to the $\Gamma_7^{1,2}$ orbital. However, the relative intensity of the t_{2g}-related peak A for Sr$_4$Ru$_2$O$_9$ in Fig. 2 is greater at the L_2 edge than at the L_3 edge. Once again we see that the predictions of the single-particle picture are not sufficient to explain the observed $4d^3$ $L_{2,3}$ XAS spectrum. Comparing now the Ru(V) with the Ru(IV) systems, we note that on increasing the Ru valence, the double-peaked L_2 and L_3 edges are shifted by 1.5 eV to the higher energy. This shift is very similar to those observed in the Ni or Cu-$L_{2,3}$ XAS spectra on going from Ni(II) to Ni(III) or from Cu(II) to Cu(III) in $3d$ TM systems.[17]

In order to understand the observed XAS spectra in detail we have performed a series calculations within the CFMC approach, which are presented in the next section.

IV. CALCULATIONS

The Hamiltonian for the crystal-field-multiplet calculations is written as

$$H = H_{av} + H_{MS}. \qquad (1)$$

H_{av} gives the average energy and does not contribute to spectral splittings, while H_{MS} includes all contribution to splittings given by

$$H_{MS} = \mathbf{L} \cdot \mathbf{S}(2p) + H_{CCF} + \mathbf{L} \cdot \mathbf{S}(4d) + g(ij). \qquad (2)$$
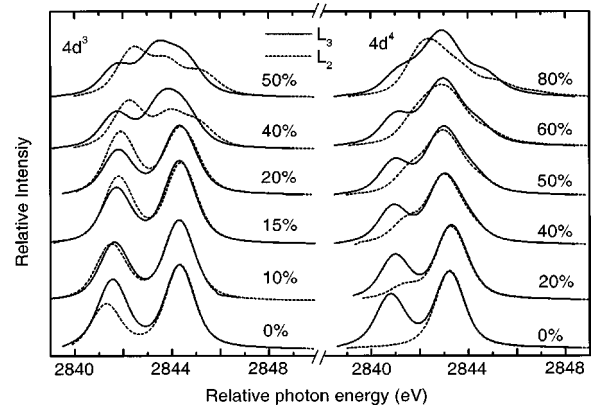

FIG. 3. Theoretical multiplet spectra at the L_3 (solid lines) and L_2 (dashed lines) edges for (right panel) Ru $4d^4$ configuration with $10Dq = 2.5$ eV, and (left panel) Ru $4d^3$ configuration with $10Dq = 2.7$ eV. The values of the Slater integrals (given as a percentage of their atomic values) used for both configurations are also given.

For $4d$ TM compounds the large spin-orbit splitting of the $2p$ core hole merely separates the L_3 and the L_2 edges into two groups of spectra, and does not contribute to the splittings for each edge. The spectral structures are determined by the cubic crystal field, H_{CCF}, the two-electron Coulomb term, $g(i,j)$, as well as the spin-orbit splitting of the $4d$ electron, $\mathbf{L} \cdot \mathbf{S}(4d)$. The $g(i,j)$ term is required to account for "multiplet effects" and its importance will be emphasized in the following. The radial part of $g(i,j), R^k$, is divided into a direct Coulomb term F^K and an exchange term G^K— the so-called Slater integrals. In this work the degree of reduction of the Slater integrals from their atomic values is taken as a free parameter to simulate the effects of hybridization in solids, known as nephelauxetic effects.[18]

The right panel of Fig. 3 shows the calculated Ru-L_3 (solid line) and Ru-L_2 (dashed line) XAS spectra for a $4d^4$ Ru(IV) configuration using $10Dq = 2.5$ eV. The L_2 edge has been shifted by the $2p$ spin-orbit splitting of 131 eV and multiplied by 2.9. The atomic value of the Slater integrals are $F^2(pd) = 2.1$ eV, $G^1(pd) = 1.8$ eV, and $G^3(pd) = 1.0$ eV, and the $4d$ spin-orbit splitting is 0.146 eV. Each calculated spectrum is labeled with the value of the Slater integrals in percent (%) of the atomic values. In the extreme case that the Slater integrals are reduced to zero, i.e., neglecting the $g(i,j)$ term (bottom-most spectrum in the right panel of Fig. 3), the peak A observed in experiment at the low-energy side of the L_2 XAS spectrum for Ru $4d^4$ is absent, and the CFMC approach arrives at the same result as the single-particle model shown in Fig. 1. Thus it is clear that in the absence of the two-electron Coulomb interaction, the $4d$ spin-orbit coupling results in the closing of the t_{2g} channel at the L_2 edge for the $4d^4$ configuration. However, as the Slater integrals are switched on, the t_{2g} channel at the L_2 edge becomes allowed and its intensity increases with increasing Slater integrals, while the t_{2g}-related spectral weight at the L_3 edge decreases. This means that for the L_2 edge in $4d^4$ systems the $4d$ spin-orbit coupling suppresses the t_{2g}-related intensity, while the Slater integrals result in an intensity transfer from the e_g- to t_{2g}-related peak. The combination of the $4d$ spin-orbit coupling and the Slater integrals thus results in a weak t_{2g}-related peak at the L_2 edge. Comparison

of the data of Figs. 2 and 3 (right panel) gives best agreement for RuO_2 and Sr_2RuO_4 with the Slater integrals at about 40% of their atomic value. A further increase of the Slater integrals results in the overestimation of the multiplet effects, leading to unrealistically broad theoretical spectra. As can be seen at the top of Fig. 3 (right panel), for the highest Slater integral values considered, the degeneracy of the t_{2g} and e_g states is lifted, resulting in a triple-peaked structure. These values of the Slater integrals are reasonable in the light of a previous study of Nb(V), Mo(VI), and Ru(III) systems with $L_{2,3}$ XAS.[8]

The theoretical spectra for the $4d^3$ configuration are shown in the left panel of Fig. 3 using $10Dq = 2.7$ eV. In this case the L_2 edge has been shifted and multiplied by 2.6 for comparison. Since the covalency increases with increasing Ru valence, the Slater integrals have to be drastically reduced to as little as 15% of their atomic values in order to reproduce the experimental spectrum of $Sr_4Ru_2O_9$ as regards the intensity ratio $I(t_{2g})/I(e_g)$ and the energy shift with respect to the Ru(IV) compounds. However, importantly, the Slater integrals are not zero. On reduction of the Slater integrals to 0%, the relative intensity ratio of $I(t_{2g})/I(e_g)$ is larger at L_3 than L_2 giving again the same results as the single-particle scenario sketched in Fig. 1. An approximately equal $I(t_{2g})/I(e_g)$ ratio at the L_2 and the L_3 is found for a reduction to 10%. The extent to which the Slater integrals need to be reduced is larger for the $4d$ than for the $3d$ TM elements due to the more delocalized nature of the $4d$ electronic states. As in the $4d^4$ case, overly large Slater integrals (for $4d^3$ meaning $>20\%$) lead to the multiplet-induced breakdown of the crystal-field terms t_{2g} and e_g, and, consequently, a triple-peak structure is clearly observed for the both L_2 and L_3 edges.

In the foregoing we discussed that the Slater integrals have little influence on the $L_3:L_2$ ratio, while the $4d$ spin-orbit coupling has a large effect on it. In increasing the value of $\mathbf{L} \cdot \mathbf{S}(4d)$ only slightly from 0 to 0.14 eV, the $L_3:L_2$ ratio increases significantly from 2:1 to 3:1. The experimental $L_3:L_2$ ratio is 2.15:1 for both Ru(IV) compounds and is close to 2:1 for the Ru(V) system. This is assigned in the latter case to the quenching of the orbital moment due to the strong covalency. Further work is needed to understand the influence of the individual parameters, $\mathbf{L} \cdot \mathbf{S}(4d)$, $4d$-$4d$ coupling (Slater integrals), $10Dq$ (4Ds for tetragonal distortion) as well as the role of ligand hole $4d^{n+1}\underline{L}$ configuration, on the detailed spectral shape. Here we wish to stress that not only the $4d$ spin-orbit coupling, but also the Slater integrals determine the details of spectral structure at the both the L_2 and the L_3 edges.

We now finish the paper with the presentation and discussion of the O-K XAS spectra for the same Ru (IV) and Ru(V) systems. In O-K XAS spectra, the correlation effects are much weaker than in the TM-$L_{2,3}$ XAS spectra, and meaningful comparison between the former and the results of band-structure calculations is plausible.[19–21] Therefore, O-K XAS spectra are usually studied in order to explore the number and location of O $2p$ holes induced by covalence or doping, and the crystal-field splitting in the ground state. Figure 4 shows the O-K XAS spectra of the three Ru oxides under consideration. The spectral structures just above the absorption edge are assigned to unoccupied O $2p$ states
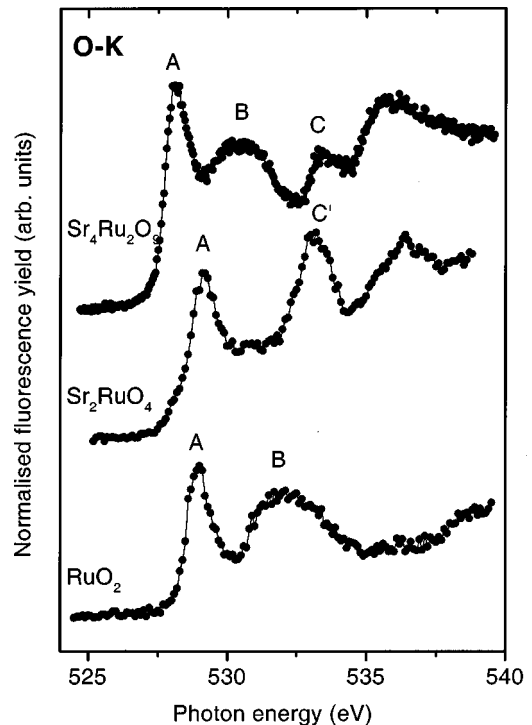

FIG. 4. Measured O-K XAS spectra of the Ru(IV) oxides RuO_2 and Sr_2RuO_4 and the Ru(V) oxide $Sr_4Ru_2O_9$. The solid lines though the data points are guides to the eye.

caused by TM-$4d$O-$2p$ covalency. For RuO_2, the first peak, A, located at 529 eV, is assigned to states hybridized with a t_{2g}-related band,[22] whereas the second peak, B, centered at ca 532 eV, is related to an e_g-derived band. This allows the derivation of the energy separation between the unoccupied portion of the t_{2g} states to the e_g states to be ca 3 eV, which is consistent with the results of band-structure calculations.[22]

In the case of Sr_2RuO_4, a similar assignment of the O-K XAS spectra can be made. However, care should be taken, as band-structure calculations[23] indicate that in the energy region 532–538 eV significant hybridization between O $2p$ and Sr $5d$ related states occurs. This has the consequence that the strong feature C' at 533.2 eV cannot be assigned to transitions into O $2p$ orbitals hybridized with the e_g-related states alone, as was suggested recently.[21]

As it possess the same O_h symmetry, the spectral features of $Sr_4Ru_2O_9$ near the O-K threshold shown at the top of Fig. 4 are very similar to those in RuO_2, except for a shift to lower energy of ca. 1 eV, consistent with the observation of the $3d$ transition-metal oxides.[17] The shift of the Ru $4d$-related states to lower energy results in a clear separation between the hybridized O $2p$/Ru $4d$ states and the states due to hybridization with Sr $5d$, denoted C in $Sr_4Ru_2O_9$: therefore, unlike Sr_2RuO_4, one can directly observe the e_g-related states in $Sr_4Ru_2O_9$. The energy separation between the unoccupied portion of the t_{2g} states and the e_g states in the Ru(V) system is ca 2.6 eV.

V. CONCLUSIONS

The correlation effects in the $L_{2,3}$ XAS spectra of $4d$ TM compounds are not as strong as those of $3d$ TM compounds, and therefore the observed spectral features in the case of O_h

symmetry reflect basically the t_{2g} and the e_g-related unoccupied electronic states. However, we show here that the correlation effects do modify significantly the spectral intensity distribution, resulting in a difference between the L_2 and the L_3 spectra.

For Ru(IV) compounds, the $4d$ spin-orbit coupling alone results in a zero transition matrix element to the t_{2g}-related states at the L_2 edge, while the Slater integrals result in intensity transfer from the e_g to t_{2g} related peak. The combination of both the $4d$ spin-orbit and correlation interactions is shown to be responsible for the observation of a distinct but weaker t_{2g}-related peak at the L_2 edge than at the L_3 edge for two representative Ru(IV) systems RuO_2 and Sr_2RuO_4. For the Ru(V) compound $Sr_4Ru_2O_9$, this combination of effects results in an intensity ratio $I(t_{2g})/I(e_g)$, which is stronger at the L_2 than the L_3 edge. The reverse would be expected from the effect of the $4d$ spin-orbit interaction alone. These observations indicate that the different L_3 and L_2 XAS spectral features in $4d$ systems are not only due to $4d$ spin-orbit coupling, but also to the effect of electronic correlation described by the Slater integrals.

Investigation of the three Ru compounds at the O-K edge revealed the following. The observed energy separation between the unoccupied t_{2g} states and the e_g states for RuO_2 of ca. 3 eV is compatible with the crystal-field splitting derived from band-structure calculations. For Sr_2RuO_4 no such conclusion is possible from the O-K XAS data due to the contributions from O $2p$/Sr $5d$ hybrid states in the same energy region as the O $2p$/Ru $4d(e_g)$ states. For the Ru(V) system $Sr_4Ru_2O_9$, the features derived from O $2p$/Ru $4d$ hybrid states are shifted by some 1 eV to lower energy. This results in a clear separation between the O $2p$/Ru $4d(e_g)$ and O $2p$/Sr $5d$ states. On going from Ru(IV) to Ru(V), both this shift to lower energy in the O-K edges and the observed shift to higher energy of the double peaks in the Ru-$L_{2,3}$ spectra follow the same pattern as is observed in the $3d$ TM oxides.[17]

Finally, the experimental and theoretical results here set up a reference for the more complicated $R_{2-x}Ce_xRuSr_2Cu_2O_{10}$ systems in which both magnetism and superconductivity coexist.

[1] F. M. F. de Groot, J. Fuggle, B. T. Thole, and G. A. Sawatzky, Phys. Rev. B **41**, 928 (1990).

[2] F. M. F. de Groot, J. Fuggle, B. T. Thole, and G. A. Sawatzky, Phys. Rev. B **42**, 5459 (1990).

[3] A. V. Pendharkar and C. Mande, Chem. Phys. **7**, 244 (1975).

[4] C. Sugiura, M. Kitamura, and S. Muramatsu, J. Chem. Phys. **84**, 4824 (1986).

[5] G. N. George, W. E. Cleland, Jr., J. H. Enemark, B. E. Smith, C. A. Kipke, S. A. Roberts, and S. P. Cramer, J. Am. Chem. Soc. **112**, 2541 (1990).

[6] C. Sugiura, M. Kitamura, and S. Muramatsu, J. Phys. Chem. Solids **49**, 1095 (1988).

[7] T. K. Sham, J. Am. Chem. Soc. **105**, 2269 (1983).

[8] F. M. F. de Groot, Z. Hu, M. F. Lopez, G. Kaindl, F. Guillot, and M. Tronic, J. Chem. Phys. **101**, 6570 (1994).

[9] Y. Maeno, H. Hashimoto, K. Yoshida, S. Nishizaki, T. Fujita, J. G. Bednorz, and F. Lichtenberg, Nature (London) **372**, 532 (1994).

[10] L. Bauernfeind, W. Widder, and H. F. Braun, Physica C **254**, 151 (1995).

[11] I. Felner, U. Asaf, Y. Levi, and O. Millo, Phys. Rev. B **55**, 3374 (1997).

[12] L. Tröger, D. Arvanitis, K. Baberschke, H. Michaelis, U. Grimm, and E. Zschech, Phys. Rev. B **46**, 3283 (1992).

[13] J. Jaklevic, J. A. Kirby, M. P. Klein, and A. S. Robertson, Solid State Commun. **23**, 679 (1997).

[14] S. Ebbinghaus and A. Reller, Solid State Ionics **101−103**, 1369 (1997).

[15] L. Walz and F. Lichtenberg, Acta Crystallogr., Sect. B: Struct. Sci. **49**, 1268 (1993).

[16] C. Dussarrat, J. Fompeyrine, and J. Darriet, Eur. J. Solid State Inorg. Chem. **32**, 3 (1995).

[17] Z. Hu, Chandan Mazumdar, G. Kandl, F. M. F. de Groot, S. A. Warda, and D. Reinen, Chem. Phys. Lett. **297**, 321 (1998).

[18] C. K. Jorgensen, *Modern Aspects of Ligand Field Theory* (North Holland, Amsterdam, 1971).

[19] M. Abbate, R. Potze, G. A. Sawatzky, and A. Fujimori, Phys. Rev. B **49**, 7210 (1994).

[20] P. Kuiper, G. Kruizinga, J. Ghijsen, G. A. Sawatzky, and H. Verweij, Phys. Rev. Lett. **62**, 221 (1989).

[21] M. Schmidt, T. R. Cummins, M. Bürk, D. H. Lu, N. Nücker, and S. Schuppler, Phys. Rev. B **53**, R14 761 (1996).

[22] K. M. Glassford and J. R. Chelikowsky, Phys. Rev. B **47**, 1732 (1993).

[23] D. J. Singh, Phys. Rev. B **52**, 1358 (1995).